

R. SKULSKI*, D. BOCHENEK*, P. WAWRZAŁA*

TECHNOLOGY, PHYSICAL PROPERTIES AND PHASE TRANSITIONS IN PMN-PT-PS CERAMICS**TECHNOLOGIA, WŁAŚCIWOŚCI FIZYCZNE I PRZEMIANY FAZOWE W CERAMICE PMN-PT-PS**

Solid solution of $(1-y)[(1-x)\text{Pb}(\text{Mg}_{1/3}\text{Nb}_{2/3})\text{O}_3 - x\text{PbTiO}_3] - y\text{PbSnO}_3$ (PMN-PT-PS) investigated in this paper is based on $(1-x)\text{PMN}-x\text{PT}$ (PMN-PT) where, with increasing x , the transition from relaxor to ferroelectric properties is observed depending on composition. PMN-PT ceramics with $0.25 < x < 0.4$ has been obtained using sol-gel method and next mixed together with PS ceramics obtained from oxides. Final sintering of ceramic samples was pressureless. We present the results of microstructure and XRD investigations, dielectric permittivity and hysteresis loops measurements vs. temperature.

Keywords: PMN-PT -PS, ferroelectric, relaxor, ceramics, sol-gel, hysteresis loop

Opisany w tej pracy roztwór stały $(1-y)[(1-x)\text{Pb}(\text{Mg}_{1/3}\text{Nb}_{2/3})\text{O}_3 - x\text{PbTiO}_3] - y\text{PbSnO}_3$ (PMN-PT-PS) jest oparty na roztworze $(1-x)\text{PMN}-x\text{PT}$ (PMN-PT) w którym, w zależności od składu ma miejsce przejście od właściwości relaksorowych do ferroelektrycznych ze wzrastającym x . Ceramika PMN-PT z $0,25 < x < 0,4$ została otrzymana metodą zolowo-żelową, a następnie wymieszana z ceramiką PS otrzymaną z tlenków. Końcowe spiekanie było spiekaniem swobodnym. Przedstawiamy rezultaty badań mikrostruktury, badań rentgenowskich, zależności przenikalności dielektrycznej i pętli histerezy dielektrycznej od temperatury.

1. Introduction

Investigated material has general formula $A[(B'B'')B''']\text{O}_3$ and belongs to perovskite type materials. Chemical composition can also be presented as $(1-u-y)\text{AB}'\text{O}_3 - u\text{AB}''\text{O}_3 - y\text{AB}''' \text{O}_3$ or similar. Position A in the perovskite elementary cell is occupied by Pb^{2+} ions. B positions are occupied by $\text{Mg}^{2+}/\text{Nb}^{5+}$ ions with the ratio of $1/3$ and by another ions i.e. Ti and Sn with the valence equal to four. Investigated by us solid solution $(1-y)[(1-x)\text{Pb}(\text{Mg}_{1/3}\text{Nb}_{2/3})\text{O}_3 - x\text{PbTiO}_3] - y\text{PbSnO}_3$ with $y=0.1$ can be abbreviated as PMN-PT-0.1PS. The introduction of PbSnO_3 gives an additional possibility to influence on temperature dependent parameters. It means that it is possible to obtain the material with optimal parameters at the for example room temperature, or any other.

PMN is known as a classic relaxor. The maximum value of dielectric permittivity in this material for frequency about 1kHz is placed at temperature T_m about 265-275K (i.e. lower than the room temperature). We want to stress that the PMN exhibits very strong dispersion of the maximum of dielectric permittivity i.e.

T_m depends on frequency of the measuring field. During heating in PMN very slow decay of hysteresis loop take place. At the same time macroscopic structural investigations do not exhibit the presence of the phase transition at mentioned temperature range. Although these typical for relaxors properties are known from many years, the origin of them is the object of interest up to now. In the opinion of many authors the behaviors of relaxors are a consequence of an existence of microscopic polar regions (MPR) instead of normal ferroelectric domains. In contrast to normal ferroelectric domains the MPR are the separated volumes of nanometer sizes and can easy and independently rotate.

The addition of PbTiO_3 (PT) into PMN shifts T_m towards higher temperatures, and changes dielectric and electromechanical parameters and decreases the degree of diffusion of the phase transition. The solid solution of $(1-x)\text{PMN}-x\text{PT}$ was a base for manufacturing our material. In PMN-PT at the room temperature continuous transition from the relaxor to normal ferroelectric properties takes place with increasing x . At the same time temperature of maximum of real part of dielectric permittivity increases from $\sim 265\text{K}$ for $x = 0$ up to $\sim 500\text{K}$ for

* UNIVERSITY OF SILESIA, DEPARTMENT OF MATERIALS SCIENCE, 41-200 SOSNOWIEC, 2 ŚNIEŻNA STR., POLAND

$x = 0,5$ [1]. In work [1] the phase diagram of PMN-PT was presented on the base of dielectric permittivity measurements. More recently Noheda et al. [2], Singh et al. [3] and Zekria [4] improved the phase diagram of PMN-PT on the base of structural investigations. However investigations with the use of synchrotron radiation made by Ye et al. [5] showed almost zero changes of parameters of the unit cells what means that it is very hard to estimate the temperature of the phase transition. PMN-PT depending on their contents demonstrate very good electromechanical properties what is important for applications.

In this paper we have investigated $(1-y)[(1-x)\text{Pb}(\text{Mg}_{1/3}\text{Nb}_{2/3})\text{O}_3 - x\text{PbTiO}_3] - y\text{PbSnO}_3$ solid solution i.e. PMN-PT-PS abbreviated to PPP. Unlike PMN-PT we have not found the papers concerning phase diagram and dielectric properties of PMN-PT-PS. The main purpose of this paper is to obtain the ceramic samples of this material and to investigate their microstructure, structure and dielectric properties vs. temperature. There are two aspects of our investigations. One is the additional possibility to shift the temperature T_m towards lower temperatures what is important for practical applications. The second one is the additional possibility to understand the physical phenomena in lead containing relaxor ferroelectrics with perovskite structure.

2. Experimental

The technology consisting of several steps have been used to obtain the samples of PMN-PT-PS. PMN, PT and in the next step PMN-PT specimens have been synthesized using sol-gel technology similar to the one described in the work of Jiwei [6]. Technology and properties of our PMN-PT samples have been described elsewhere [7]. The results of investigations of d.c. and a.c. conductivity are presented in [8].

PbSnO_3 has been obtained from oxides of PbO (with excess of 3.5%mol) and SnO_2 . Initial oxides were milled and mixed using FRITSCH mill (15h in ethyl alcohol). The last step in manufacturing of PbSnO_3 was calcination at $850^\circ\text{C}/4\text{h}$.

The resultant powders of PMN-PT and PS were mixed in stoichiometric proportion and calcined at 950°C for 5h. Next, the pellets with diameter of 10mm were formed and sintered at $1250^\circ\text{C}/3\text{h}$. In such a way the compositions of $(1-y)[(1-x)\text{Pb}(\text{Mg}_{1/3}\text{Nb}_{2/3})\text{O}_3 - x\text{PbTiO}_3] - y\text{PbSnO}_3$ with $x=0.25, 0.28, 0.31, 0.34, 0.37, 0.4$ and $y=0.1$ have been obtained. Throughout the paper we use also the following abbreviations: $x=0.25$ PPP-1; $x=0.28$ PPP-2; $x=0.31$ PPP-3; $x=0.34$ PPP-4; $x=0.37$ PPP-5; $x=0.4$ PPP-6.

During the last step of technology the silver paste electrodes have been put on both surfaces of the samples.

For SEM investigations the ceramic samples of PMN-PT-PS have been broken and next, a thin layer of carbon was spread on the examined surface.

X-ray diffraction patterns (XRD) have been obtained using a Siemens D5000 diffractometer and CuK_α filtered radiation with a 0.02 deg step.

The investigation of dielectric permittivity $\epsilon'(T)$ and $\tan\delta(T)$ were carried out using a BM2817 LCR Meter.

Hysteresis ($P - E$) loops were investigated using a Sawyer-Tower circuit and a HEOPS-5B6 Matsusada Inc. precision high voltage amplifier. Data were stored on a computer disc using an A/D, D/A transducer card.

3. Results and discussion

Obtained SEM images for sample with the biggest and the smallest grains (PPP-3 and PPP-6 respectively) are presented in Fig. 1. It also can be stated from this figure that the large heterogeneity of grain sizes takes place.

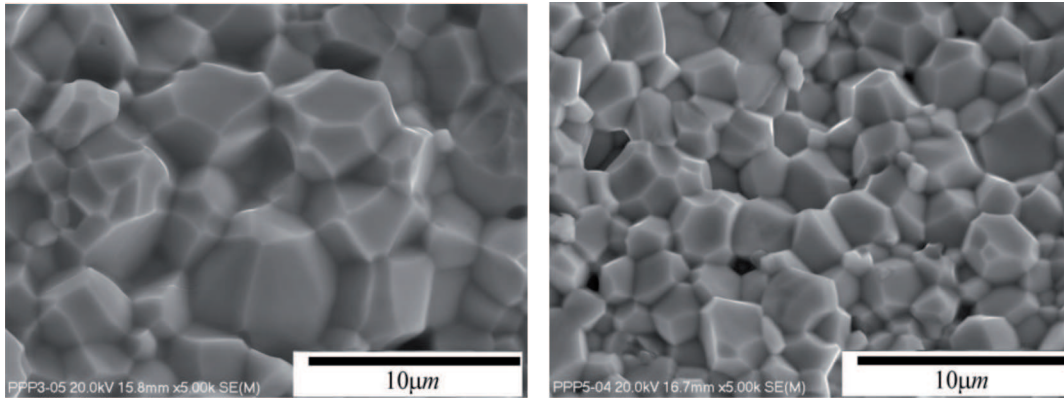


Fig. 1. SEM images of PMN-PT-PS ceramics, in which the grains are the biggest and the smallest: a) 0.621PMN-0.279PT-0.1PS (PPP-3); b) 0.567PMN-0.333PT-0.1PS (PPP-6)

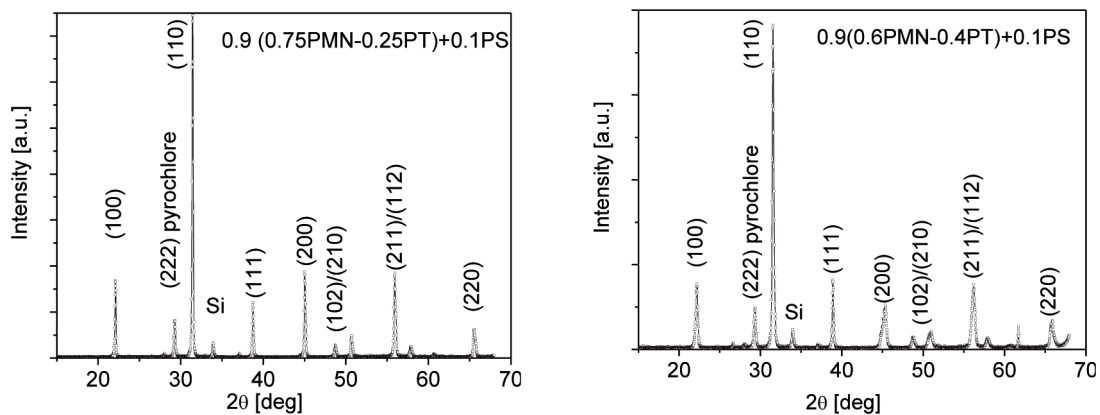


Fig. 2. XRD patterns for PPP-1 and PPP-6. Line described as Si is related to the fact, that PMN-PT-PS powder was investigated on the surface of Si rod

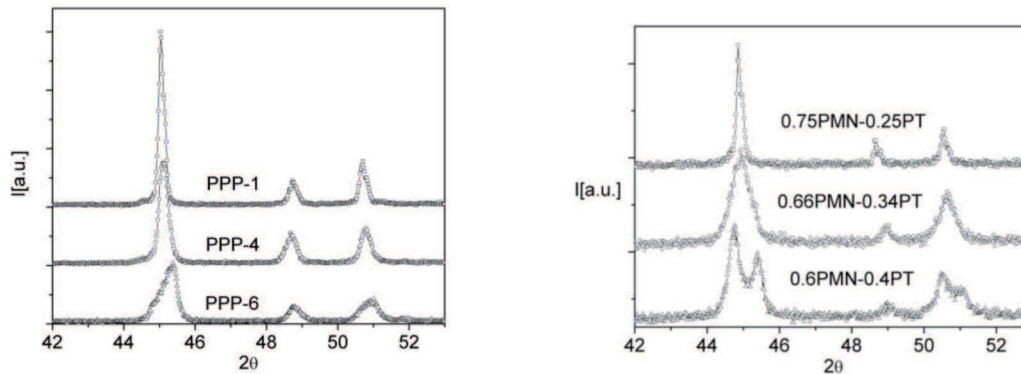


Fig. 3. The comparison between selected parts of XRD patterns of PPP ceramics (a) and PMN-PT ceramics (without tin) (b)

Results of XRD investigations are presented in Fig. 2 for PPP-1 and PPP-6. Line described as Si is related to the fact, that PMN-PT-PS powder was investigated on the surface of Si rod. It is also seen the line connected with the presence of the useless pyrochlore phase. In Fig. 3 we present the changes in the shape of line (200) of the perovskite phase with increase in content of PbTiO_3 in investigated PPP ceramics and in PMN-PT ceram-

ics for comparison. In the case of PMN-PT changes in the shape of (200) line clear suggest that with increasing x the morphotropic phase transition between $x=0.25$ and $x=0.4$ takes place and as a result 0.6PMN-0.4PT is tetragonal. In the case of PMN-PT-PS with increasing x the morphotropic phase transition between $x=0.25$ and $x=0.4$ probably also takes place, however it is not so clear like in PMN-PT.

The results of investigation of dielectric permittivity $\varepsilon''(T)$ for all investigated samples are presented in Fig. 4. Temperature T_m at which $\varepsilon''(T)$ has a maximum linearly depends on x what is presented in Fig. 5 and is compared with data for PMN-PT from work [9]. It can be stated from this figure that the temperatures T_m for obtained

PPP samples are about 40K lower than for PMN-PT ceramics with the same PMN/PT ratio. It is also seen that with increasing x the diffusion of maximum of dielectric permittivity decreases and as a result the T_m temperature practically does not depend on frequency.

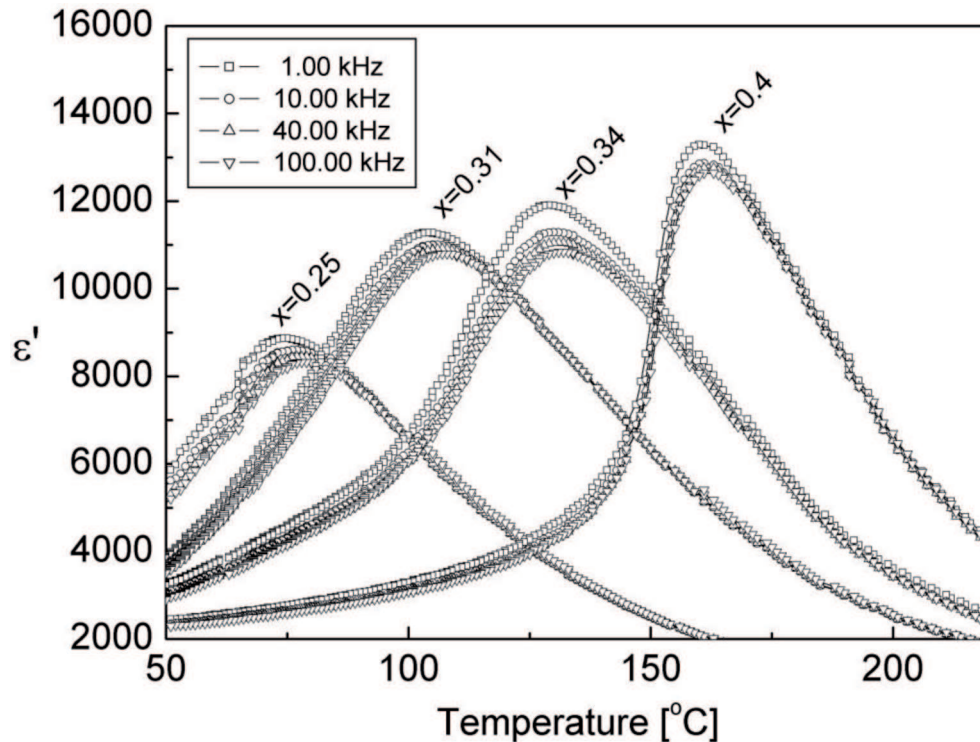


Fig. 4. Dependencies $\varepsilon''(T)$ for all investigated samples

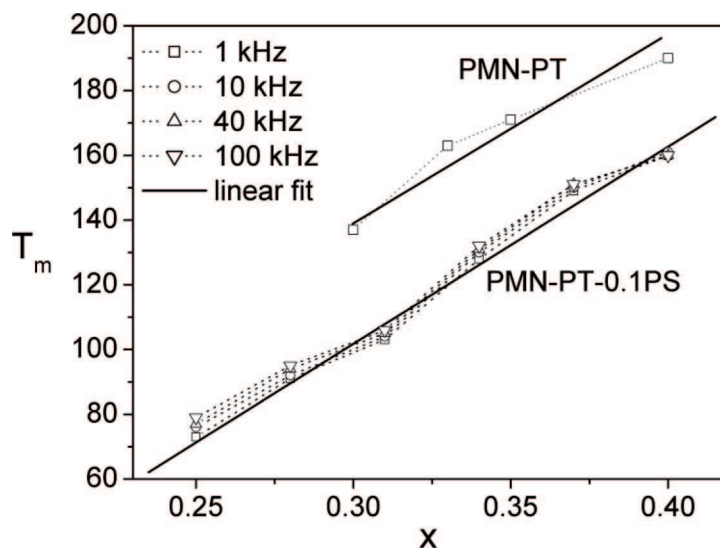


Fig. 5. The dependency of the temperature T_m at which $\varepsilon''(T)$ has its maximum on x for investigated PMN-PT-PS ceramics. The upper points and line are the data for PMN-PT from work [9]

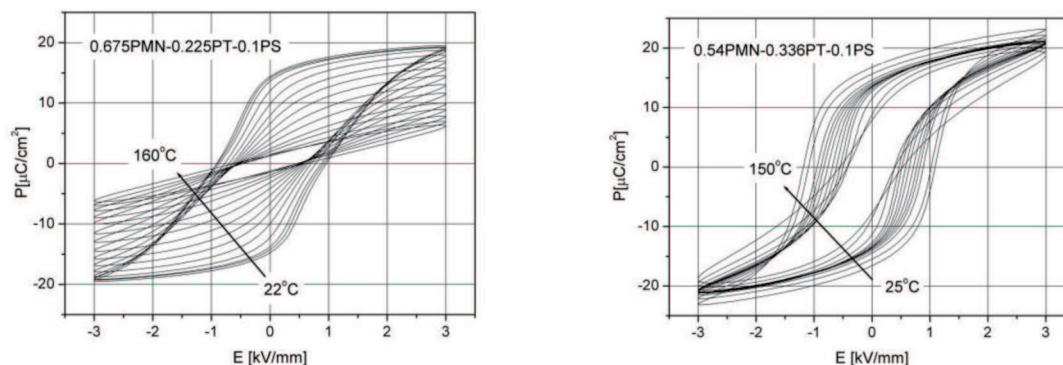


Fig. 6. Hysteresis loops for PPP-1 (a) and PPP-6 (b) at various temperatures. Frequency 1 Hz

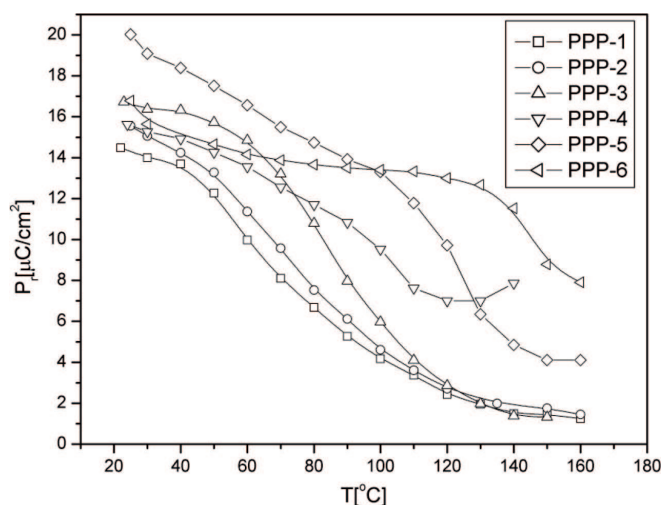


Fig. 7. The dependency of remnant polarization P_r on temperature for all investigated samples

Hysteresis loops for PPP-1 and PPP-6 obtained at various temperatures are presented in Fig. 6. The dependencies $P_r(T)$ for all investigated samples are presented in Fig. 7. The shift between temperatures of transition obtained by various methods is typical for relaxor ferroelectrics. Good method of identification of the temperature of phase transition is to calculate a derivative of $P_r(T)$. Comparing such obtained derivative (not presented in figures) with data from Fig. 4 and Fig. 5 it is possible to say, that the phase transition from relaxor ferroelectric to paraelectric phase take place at temperatures about 20K lower than T_m .

4. Conclusions

The microstructure of obtained PMN-PT-PS samples exhibits well shaped grains, a little bigger than in PMN-PT without tin. XRD patterns show that the amount of unwanted pyrochlore phase is higher than in PMN-PT samples. It is observed linear shift of T_m with increasing x like in PMN-PT. In the case of PMN-PT-PS

the morphotropic phase transition between $x=0.25$ and $x=0.4$ is not so clear like in PMN-PT.

The most suitable for practical applications seems to be the ceramics of $0.9(0.75\text{PMN}-0.25\text{PT})+0.1\text{PS}$ since the temperature T_m is the lowest between investigated samples. Taking into account that the phase transition temperature calculated from $P_r(T)$ is about 20K lower than T_m this composition seems to be the best for applications for example at pulse capacitors.

Acknowledgements

Work supported by Polish Grant N N507 480237.

REFERENCES

- [1] T.R. Shrouf, Z.P. Chang, N. Kim, S. Markgraf, Dielectric behavior of single crystals near the $(1-x)\text{PbMg}_{1/3}\text{Nb}_{2/3}\text{O}_3-x\text{PbTiO}_3$ morphotropic phase boundary, *Ferroelectr. Lett.Sect.* **12**, 63 (1990).
- [2] B. Noheda, D.E. Cox, G. Shirane, J. Gao, Z.-G. Ye, Phase diagram of the ferroelectric relaxor $(1-x)\text{PbMg}_{1/3}\text{Nb}_{2/3}\text{O}_3-x\text{PbTiO}_3$, *Phys. Rev. B*, **66**, 0541041-0541049 (2002).
- [3] A.K. Singh, D. Pandey, Evidence for MB and MC phases in the morphotropic phase boundary region of $(1-x)\text{PbMg}_{1/3}\text{Nb}_{2/3}\text{O}_3-x\text{PbTiO}_3$: a Rietveld study, *Phys. Rev. B*, **67**, 641021-6410212 (2003).
- [4] D. Zekria, A.M. Glazer, Automatic determination of the morphotropic phase boundary in lead magnesium niobate titanate $\text{Pb}(\text{Mg}_{1/3}\text{Nb}_{2/3})_{(1-x)}\text{Ti}_x\text{O}_3$ within a single crystal using birefringence imaging, *J. Appl. Cryst.* **37**, 143-149 (2004).
- [5] Z.-G. Ye, Y. Bing, J. Gao et al., Development of ferroelectric order in relaxor $(1-x)\text{Pb}(\text{Mg}_{1/3}\text{Nb}_{2/3})\text{O}_3-x\text{PbTiO}_3$ ($0 < x < \sim 0.15$), *Phys. Rev. B* **67**, 104104 (2003).
- [6] Z. Jiwei, S. Bo, Z. Liangying, Y. Xi, Preparation and dielectric properties by sol-gel derived PMN-PT powder and ceramic, *Materials Chemistry and Physics*, **64**, 1-4 (2000).

- [7] R. Skulski, P. Wawrzła, D. Bochenek, K. Ćwikiel, Dielectric and electromechanical behaviors of PMN-PT ceramic samples, *Journal of Intelligent Material Systems And Structures*, **18**, 1049-1056 (2007).
- [8] R. Skulski, P. Wawrzła, J. Korzekwa, M. Szymonik, The electrical conductivity of PMN-PT ceramics, *Archives of Metallurgy and Materials*, **54**, 717-723 (2009)
- [9] X. Yhang, F. Fang, Study of the structure and dielectric relaxation behavior of $\text{Pb}(\text{Mg}_{1/3}\text{Nb}_{2/3})\text{O}_3\text{-PbTiO}_3$ ferroelectric ceramics *J. Mater. Res.* **14**, 4581-4586 (1999).

Received: 21 April 2011.